Natriuretic peptide receptor C contributes to disproportionate right ventricular hypertrophy in a rodent model of obesity-induced heart failure with preserved ejection fraction with pulmonary hypertension

Vineet Agrawal[1] , Niki Fortune[2], Sheeline Yu[2], Julio Fuentes[2], Fubiao Shi[1], David Nichols[2], Linda Gleaves[2], Emily Poovey[2], Thomas J. Wang[1], Evan L. Brittain[1], Sheila Collins[1], James D. West[2] and Anna R. Hemnes[2]

[1]Division of Cardiology, Vanderbilt University Medical Center, Nashville, TN, USA; [2]Division of Allergy, Pulmonary, and Critical Care Medicine, Vanderbilt University Medical Center, Nashville, TN, USA

Abstract

Heart failure with preserved ejection fraction (HFpEF) currently has no therapies that improve mortality. Right ventricular dysfunction and pulmonary hypertension are common in HFpEF, and thought to be driven by obesity and metabolic syndrome. Thus, we hypothesized that an animal model of obesity-induced HFpEF with pulmonary hypertension would provide insight into the pathogenesis of right ventricular failure in HFpEF. Two strains of mice, one susceptible (AKR) and one resistant (C3H) to obesity-induced HFpEF, were fed high fat (60% fat) or control diet for 0, 2, or 20 weeks and evaluated by cardiac catheterization and echocardiography for development of right ventricular dysfunction, pulmonary hypertension, and HFpEF. AKR, but not C3H, mice developed right ventricular dysfunction, pulmonary hypertension, and HFpEF. *NPRC*, which antagonizes beneficial natriuretic peptide signaling, was found in RNA sequencing to be the most differentially upregulated gene in the right ventricle, but not left ventricle or lung, of AKR mice that developed pulmonary hypertension and HFpEF. Overexpression of *NPRC* in H9C2 cells increased basal cell size and increased expression of hypertrophic genes, *MYH7* and *NPPA*. In conclusion, we have shown that *NPRC* contributes to right ventricular modeling in obesity-induced pulmonary hypertension-HFpEF by increasing cardiomyocyte hypertrophy. *NPRC* may represent a promising therapeutic target for right ventricular dysfunction in pulmonary hypertension-HFpEF.

Introduction

Pulmonary hypertension due to left heart disease (PH-LHD) is the most common form of pulmonary hypertension (PH). Among the various etiologies of PH-LHD, heart failure with preserved ejection fraction (HFpEF) represents a growing subset of these patients.[1] Notably, 80% of patients with HFpEF have concomitant PH, and the presence of PH in HFpEF (PH-HFpEF) independently increases morbidity and mortality.[2,3] Recent studies suggest a major cause of

morbidity and mortality in PH-HFpEF is right ventricular (RV) failure, occurring independent of the severity of PH.[4,5] Therapies targeting pathways known to affect pulmonary vascular and left ventricular remodeling have largely been

Corresponding author:
Vineet Agrawal, Division of Cardiology, Department of Medicine, Vanderbilt University School of Medicine, T1218 Medical Center North, 1161 21st Avenue South, Nashville, TN 37232, USA.
Email: vineet.agrawal@vumc.org

neutral or harmful in PH-HFpEF,[6–11] but no therapies to date have targeted adverse RV remodeling directly in PH-HFpEF. This is, in part, due to poor understanding of the pathophysiology of RV failure in HFpEF.[12]

Understanding the mechanisms contributing to adverse RV remodeling in HFpEF has been limited by the relative lack of pre-clinical animal models of RV failure in PH-HFpEF.[13] Human studies have shown that co-existing obesity and metabolic syndrome independently contribute to worsening RV function[14,15] as well as development of HFpEF with pulmonary vascular remodeling.[8] Thus, to better understand the mechanisms underlying maladaptive RV remodeling in PH-HFpEF, we used a validated animal model of obesity-induced PH-HFpEF[16] to study early pathways that contribute to RV remodeling. Using a second rodent strain resistant to obesity-induced PH-HFpEF,[16] we aimed to identify unique signals that contribute to the development of obesity-induced PH-HFpEF.

Methods

All animal studies were approved by the Vanderbilt University Medical Center IACUC (protocol M1800073).

Animal studies

Male mice, approximately eight weeks of age, were purchased from Jackson Laboratories. Equal numbers of AKR and C3H mice ($n = 8$ for each time point and group) were fed either a high fat diet chow consisting of 60% lard content (BioServ F3832, San Diego, CA) or a nutrient matched control diet (BioServ F4031, San Diego, CA). At 0, 2, and 20 weeks, mice underwent echocardiography and cardiac catheterization prior to sacrifice. A subset of mice ($n = 5$ in each group) underwent echocardiography and cardiac catheterization, while another subset ($n = 3$ in each group) were sacrificed for histologic analysis of tissue.

Echocardiography

Echocardiography was completed as previously described.[17] Briefly, mice were anesthetized with 2–3% isoflurane. Depilatory cream was applied to the thorax. Mice were then placed on heated table (37°C) in supine position. Using the VisualSonics Vevo700 platform and 707B transducer (30 MHz), images were acquired using 2-D B-mode, M-mode, and Doppler mode. Traditional parasternal long and short axis views were obtained, and modified parasternal long axis and apical views were used to measure RV parameters.

Cardiac catheterization

At 0, 2, and 20 weeks after starting diets, mice were anesthetized with 2–3% isoflurane and orotracheally intubated with 22 g catheter. Animals were mechanically ventilated at 18 cc/kg with vaporized isoflurane general anesthesia. Mice

were positioned supine, ventral side up on a heated operating table. A vertical incision over the abdomen was made and cautery was used to cut the diaphragm and expose the heart. A 1.4 French Mikro-tip catheter was directly inserted into the left ventricle for measurement of pressure and volume within the left ventricle. Afterwards, the catheter was removed and directly inserted into the right ventricle. Hemostasis of the left ventricle was ensured prior to catheterization of the right ventricle to ensure no effect of volume loss on findings. Hemodynamics were continuously recorded with a Millar MPVS-300 unit coupled to a Powerlab 8-SP analog-to-digital converter acquired at 1000 Hz and captured to a Macintosh G4 (Millar Instruments, Houston, TX). Mice were then sacrificed with cervical dislocation and tissues (left and right ventricle) were measured and flash-frozen in liquid nitrogen. Whole hearts from a subset of mice in each group were placed in 10% neutral buffered formalin for histologic sectioning and analysis. Transpulmonary gradient was calculated by subtracting the left ventricular end-diastolic pressure from the mean pulmonary arterial pressure, which was estimated as 60% of the RV systolic pressure.[18] Pulmonary vascular resistance was calculated in Wood units as the ratio of transpulmonary gradient to cardiac output (measured by echo as the product of velocity time integral and aortic cross-sectional area).

Lung weight measurement

After cardiac catheterization, mice were sacrificed and the lungs were harvested at the level of the bifurcation of the mainstem bronchus. Lung congestion was measured by the ratio of wet to dry weight of each lung.[19] Tissue was then weighed and dehydrated in an oven at 60°C for 1 h. Tissue was weighed at 30 min and 1 h to ensure tissue was entirely dry.

Histologic analysis

Hearts were harvested from mice and immediately either placed in 10% neutral buffered formalin or Optimal Cutting Temperature medium for processing, sectioning, and staining with hematoxylin/eosin (H&E) and Masson's Trichrome stains at three different levels. Only slides with complete short axis views of the right and left ventricle were used for analysis. Fibrosis was quantified using ImageJ to measure area of fibrosis on Masson's Trichrome stains using the Colour Deconvolution plugin. Oil Red O stain was completed as previously described[20] on frozen sections, and percentage of tissue with lipid deposition was quantified using ImageJ and the Colour Deconvolution plugin. Lung tissue were first perfused through the trachea with agarose and then fixed in formalin for sectioning and staining with H&E.

Immunofluorescence

Slides were deparaffinized and underwent heat antigen retrieval for 20 min in Tris EDTA pH 9 antigen retrieval buffer.

Samples were blocked for 2 h in 10% goat serum and 1% bovine serum albumin (BSA) prior to incubation in primary antibody overnight in 0.5% BSA. They were then incubated in secondary antibody diluted in phosphate buffered saline prior to mounting with Vectashield 4',6-diamidino-2-phenylindole DAPI (Vector Laboratories, Burlingame, CA). Images were then taken on the Nikon Eclipse Ti confocal microscope (Nikon USA, Melville, NY). Cell staining was conducted on chamber slides. Cells were washed in ice cold phosphate buffered saline PBS and fixed in 4% paraformaldehyde for 10 min prior to permeabilizing with 0.1% Triton X in PBS for 10 min. Cells were blocked for 30 min in blocking buffer as above and incubated in primary antibody in 0.5% BSA for 1 h, followed by secondary antibody for 1 h. Cell slides were mounted in Vectashield DAPI and imaged as above. Antibodies used included: alpha smooth muscle actin (Abcam, ab5694) 1:100, natriuretic peptide clearance receptor C (NPRC) (Novus Biologics, 31365) 1:50, troponin-T (Abcam, ab10214) 1:100, and Alexa Fluor 488 or 594 conjugated secondary 1:500 goat anti-rabbit IgG (Thermo Fisher Scientific).

Western blot

NPRC antibody (Novus Biologics, 31365) was used at a concentration of 1:1000 diluted in 5% milk, Tris buffered saline TBS, and 0.1% Tween 20. Secondary antibody was then used at 1:5000 dilution. Bands were detected using the SuperSignal Western Pico Chemiluminescent Substrate (Thermo Scientific, Waltham, MA) and imaged using the BioRad ChemiDoc Touch System (Bio Rad, Hercules, CA).

RNA isolation and Reverse Transcription PCR

RNA was isolated using RNAeasy kit (Qiagen, Hilden, Germany). Reverse transcription was completed using Quantitect Reverse Transcriptase Kit (Qiagen, Hilden, Germany). Thereafter, quantitative PCR was completed using SYBR Green Master PCR Mix (Applied Biosystems, Foster City, CA) and primer pairs on the QuantStudio 3 PCR machine (Applied Biosystems). PCR primers used included (5'–3'): *NPR3 Mus musculus F- ACACGTCTGCCTA CAATTTCG, R- GCACACATGATCACCACTCG; HPRT Mus musculus F-TGCTCGAGATGTCATGAAGGAG, R-TTTAATGTAATCCAGCAGGTCAGC; NPPA Rattus norvegicus F- ATCCCGTATACAGTGCGGTG, R- CTCC TCCAGGTGGTCTAGCA; MYH7 Rattus norvegicus F- TGGCACCGTGGACTACAATA, R- TACAGGTGCA TCAGCTCCAG; NPR3 Rattus norvegicus F- GGAC CTGGACGACATAGTGC; R- CCACGAGCCATCTCCGT AAG; HPRT Rattus norvegicus F-TGCTCGAGATGTC ATGAAGGA, R-TCCAACACTTCGAGAGGTCC*

RNA sequencing

RNA isolated from the right ventricle at 0 and 2 weeks from mice was submitted for RNA sequencing by the Vanderbilt

Technologies for Advanced Genomics Core at Vanderbilt University Medical Center. All samples with RNA integrity number RIN values greater than 6 were submitted for sequencing analysis. Experimental conditions included four or five replicates of a total of eight groups: two mouse strains (AKR vs C3H), two experimental groups (control diet vs high fat diet), and two time points (0 and 2 weeks). RNA sequencing was performed on an Illumina HiSeq system with a paired-end mRNA library prep, PE-150, with 30 million reads. Initial alignment and quantification of sequences was performed using the Partek Flow package. STAR 2.5.3a was used to align RNA-Seq reads, with quantification to Ensembl Transcripts Release 83 using Partek E/M. Reads were normalized to total count. Approximately 77% of all reads aligned to genes. A total of 22,232 genes were identified with at least one read in each sample. Genes with fewer than four reads per million were filtered out, yielding 1452 genes. To remove the effect of diet alone, genes with similar changes between diets in both mouse strains (AKR high fat vs control diet, C3H high fat vs control diet) were filtered. Additionally, genes were filtered for those that had a statistically significant ($p < 0.05$), >1.5 fold change difference between mouse strains in response to high fat diet (AKR vs C3H high fat diet), resulting in a total of 42 differentially regulated genes between AKR and C3H strains in response to high fat diet. Over-representation analysis was completed using WebGestalt (webgestalt.org) for the *Mus musculus* organism and gene ontology database, comparing against the genome-protein coding database. Multiple test adjustment was conducted using the Benjamini-Hochberg procedure and a false discovery rate threshold of 0.05 or lower was considered significant.

H9C2 cell culture and plasmid transfection

Cardiomyocyte-like H9C2 cells were cultured in Dulbecco's Modified Eagles Medium (DMEM) containing 10% fetal bovine serum (FBS). Prior to studies, they were cultured in DMEM containing 1% FBS for 48 h. A flag-tagged human *NPRC* construct was generated and confirmed by sequencing. A subset of H9C2 cells were transduced using Lipofectamine 2000 following manufacturer's recommended protocol with either plasmid containing NPRC or empty vector alone. Transduced cells underwent selection for one week with 1 mg/ml G418 (Sigma) followed by maintenance in 0.8 mg/ml G418 thereafter. Plasmid transfection was confirmed using PCR and Western blot for *NPRC*. Cells were cultured in DMEM supplemented with 10% FBS (Corning Biosciences) and G418.

Cell hypertrophy assays

H9C2 cells transduced with either empty vector or NPRC were differentiated into cardiomyocyte-like cells for 48 h. A subset of cells was fixed on chamber slides and permeabilized (as above) for immunofluorescent staining with

phalloidin (Sigma, 1:200 in PBS for 30 min) or harvested for RT-PCR in RLT buffer (Qiagen, Hilden, Germany). Cell size was measured randomly on 50 cells for a given experiment, and repeated three times. Cell area was quantified using ImageJ with a reader blinded to the experimental group. To analyze the effect of the addition of an NPRC-specific ligand, ANP-4-23,[21] on cell hypertrophy, transfected cells were treated with 200 nM of ANP-4-23 (Phoenix Pharmaceuticals, 005-26, Burlingame, CA) for 24 h prior to immunofluorescent staining and RT-PCR.

Statistical analysis

Statistical analysis was completed in the GraphPad Prism 5.0 package (GraphPad Software, La Jolla, CA) using one-way ANOVA with Tukey post-hoc test or two-way ANOVA (for muscularized artery analysis) with Bonferroni post-hoc correction. For pair-wise comparisons,

students t-test was used assuming equal variances. A threshold of $p < 0.05$ was considered significant.

Results

AKR, but not C3H, mice develop HFpEF

After 20 weeks of high fat diet, AKR mice developed biventricular hypertrophy and increased mass when compared to C3H mice (Fig. 1a–c). By echocardiography, all groups of mice demonstrated preserved ejection fraction (Fig. 1d), but only AKR mice fed high fat diet showed evidence of concentric hypertrophy of the LV and E to A velocity reversal on transmitral Doppler signals, consistent with HFpEF (Fig. 1b). By direct cardiac catheterization, AKR mice fed high fat diet, but not control diet, showed eccentric and concentric remodeling of the RV and LV (Fig. 1c). End-diastolic pressure was also selectively elevated in both the
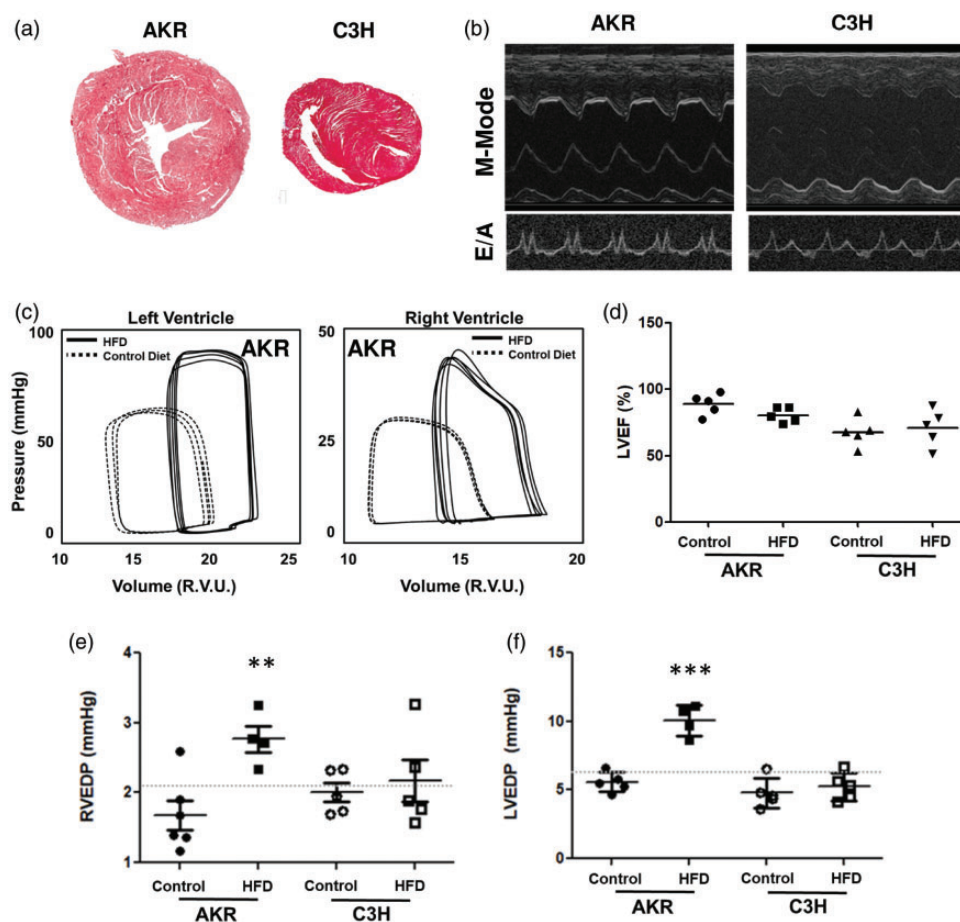

Fig. 1. Cardiac changes after 20 weeks of high fat diet. (a) H&E stain of cross-section of hearts from AKR and C3H mice fed high fat diet confirms that AKR, but not C3H, mice develop biventricular cardiac hypertrophy. (b) M-mode and transmitral Doppler echocardiography confirms ventricular hypertrophy and E to A reversal in AKR mice. (c) Representative pressure volume loops from AKR mice show biventricular concentric and eccentric remodeling consistent with HFpEF. (d) Preserved ejection fraction by echo in AKR and C3H mice. (e and f) AKR mice fed high fat diet selectively demonstrate elevated right and left ventricular end-diastolic pressures. *$p < 0.05$, **$p < 0.01$, and ***$p < 0.001$ compared to other groups. Data presented as mean $\pm$ standard deviation.

HFD: high fat diet. LVEF: left ventricular ejection fraction; LVEDP: left ventricular end-diastolic pressure; RVEDP: right ventricular end-diastolic pressure.

RV and LV of AKR mice fed high fat diet (Fig. 1e–f), suggestive of both LV and RV congestion and confirming the HFpEF phenotype.

AKR, but not C3H, mice develop PH and pulmonary vascular remodeling

After 20 weeks, histologic analysis of perfusion fixed lungs suggested that AKR mice developed more perivascular remodeling than C3H mice or either group of mice fed control diet (Fig. 2a). By catheterization, AKR mice fed high fat diet showed an increased RV systolic pressure and transpulmonary gradient, consistent with PH and pulmonary vascular remodeling (Fig. 2b). AKR mice fed high fat diet also showed evidence of lung congestion based on an increased ratio of wet to dry lung weight compared to other groups (Fig. 2c). Immunostaining of the fixed lung sections also showed that there was a significant increase in the number of muscularized small vessels ($0–25\,\mu M$) in AKR mice fed high fat diet, as well as a decrease in proportion of muscularized medium to large vessels ($50–100\,\mu M$, and $>100\,\mu M$) (Fig. 2d and e). Of note, no significant changes were noted in pulmonary vascular remodeling, hemodynamically or histologically, between any of the groups at two weeks after diet change.
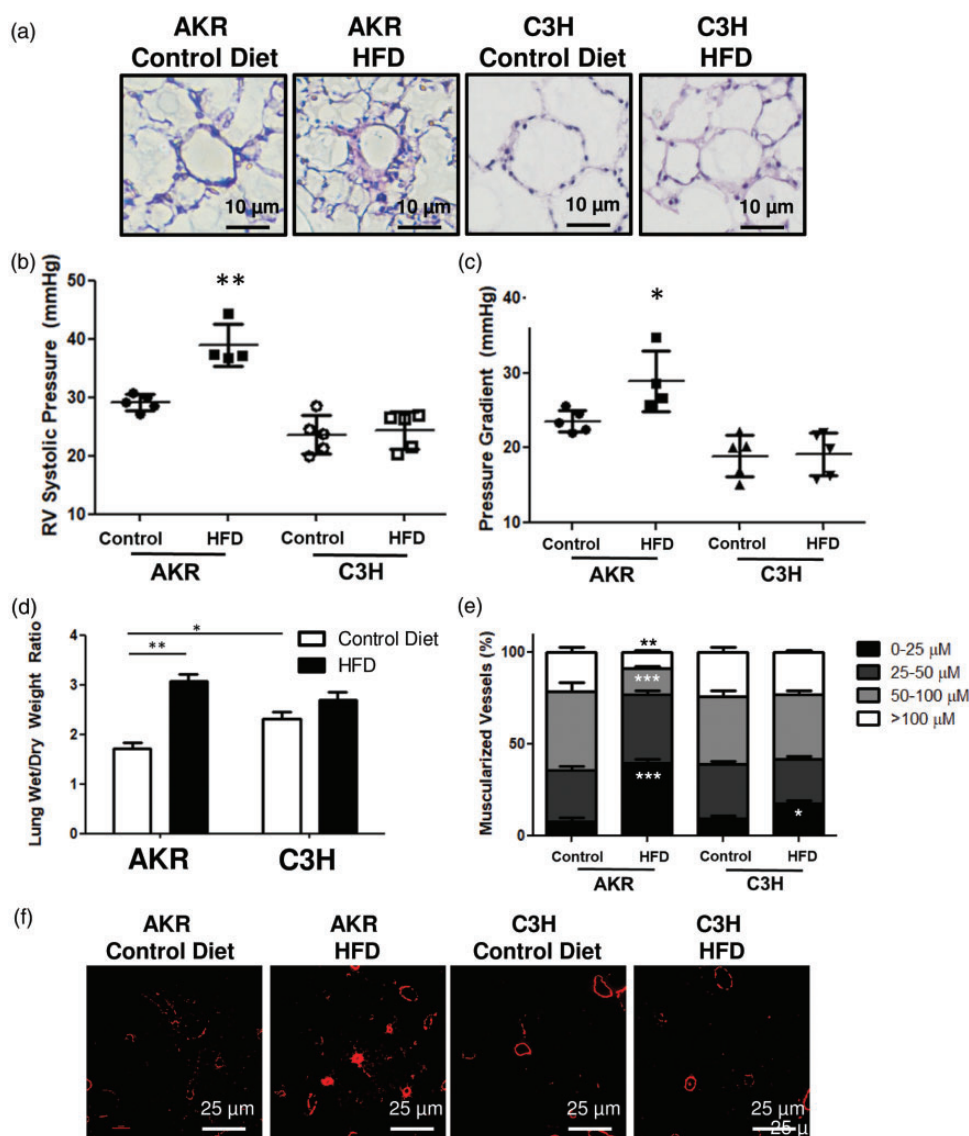

Fig. 2. Pulmonary vascular changes after 20 weeks of high fat diet. (a) AKR mice fed a high fat diet demonstrate peri-vascular remodeling. (b and c) AKR mice fed a high fat diet demonstrated elevated right ventricular systolic pressures and transpulmonary gradients. (d) AKR mice fed a high fat diet demonstrate increased lung congestion as measured by wet-to-dry lung weight. (e and f) AKR mice fed high fat diet have a greater proportion of small and medium sized muscularized vessels. $*p < 0.05$, $**p < 0.01$, and $***p < 0.001$ when compared to AKR mice fed control diet. Data presented as mean $\pm$ standard deviation.
HFD: high fat diet; RV: right ventricle.

AKR mice develop early disproportionate RV remodeling

To determine early changes that contribute to the pathogenesis of PH-HFpEF in AKR mice, mice were evaluated at an early time point (two weeks) post-initiation of diet. After two weeks of high fat diet, AKR mice fed a high fat diet had a greater free wall thickness by echocardiography and higher Fulton index compared to all other groups (Fig. 3a and c) without any significant change in RV systolic pressure or pulmonary vascular resistance (Fig. 3b), consistent with disproportionate RV hypertrophy. By histologic analysis, there was evidence of increased myocyte size, but no change in lipid accumulation or fibrosis (Fig. 3d–f).

NPRC is selectively increased in the RV of AKR mice

To determine genes and pathways differentially regulated in AKR mice fed a high fat diet, transcriptomic changes in RNA expression of all groups was assessed by RNA sequencing. After filtering out genes that showed concordant change in expression between C3H and AKR mice to account for the effect of high fat diet alone, there were 42 genes differentially expressed between C3H and AKR mice fed high fat diet (Fig. 4a). Among the genes, the most differentially expressed gene between C3H and AKR mice was *npr3*, encoding for a NPRC (Fig. 4b). Validation RT-PCR confirmed that the RV, but not LV or lung parenchyma, of AKR mice showed an increase in NPRC expression in
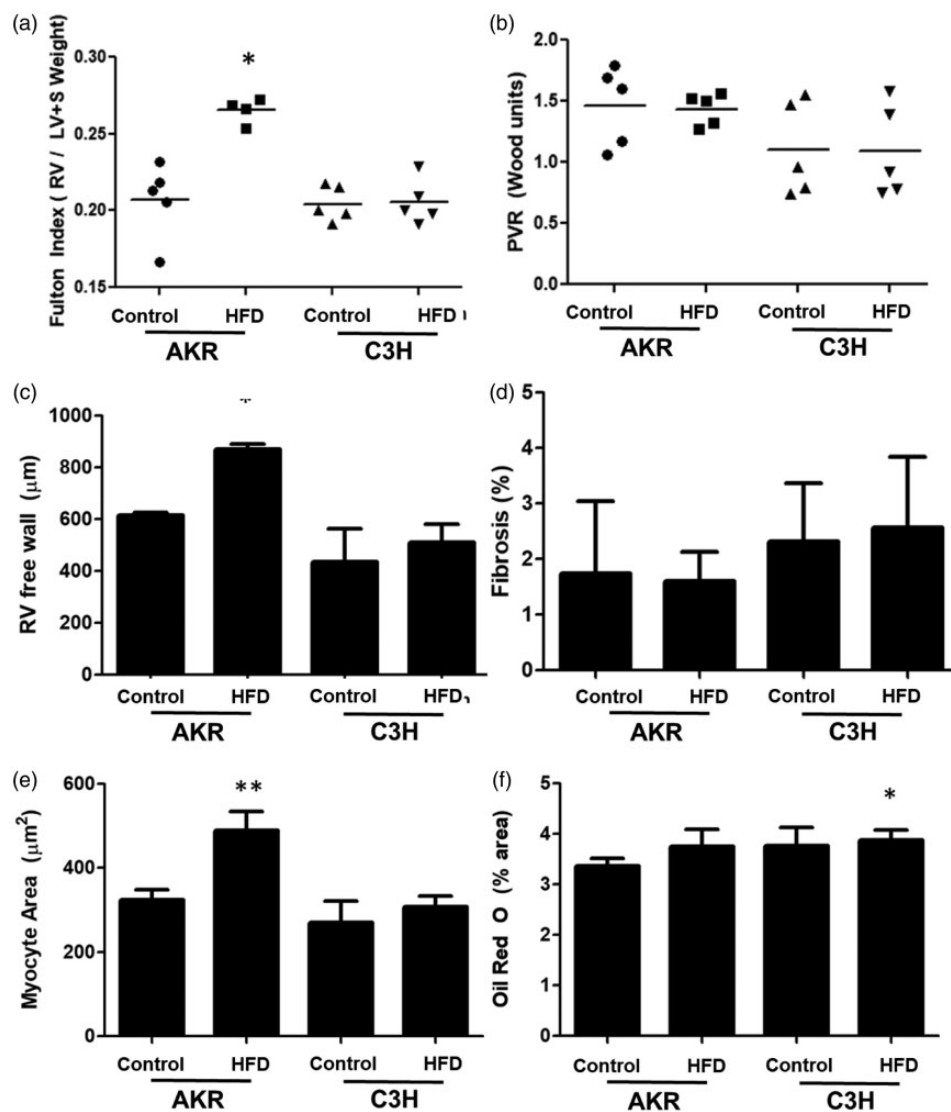

Fig. 3. Cardiac changes occurring after two weeks of high fat diet. (a) After two weeks, AKR mice fed high fat diet showed an increase in RV mass. (B) No change was noted in pulmonary vascular resistance after two weeks. (C) The free wall thickness of the RV was increased in AKR mice fed high fat diet. (D) No changes in fibrosis were noted between groups. (E) An increase in myocyte area was noted in AKR mice fed high fat diet histologically. (F) No change in lipid deposition was noted by Oil Red O stain between groups. $*p < 0.05$ and $**p < 0.01$ compared to control. Data presented as mean $\pm$ standard deviation.
HFD: high fat diet; RV: right ventricle; LV: left ventricle; PVR: pulmonary vascular resistance.

response to high fat diet (Fig. 4c). Western blot also confirmed that the increase in RV NPRC expression occurred primarily in AKR mice fed high fat diet at 2 and 20 weeks (Fig. 4d). Immunofluorescent staining also showed disproportionate increase in NPRC expression in the RV, but not LV, of AKR mice fed high fat diet with greater expression in the epicardium of the RV (Fig. 4e).

As NPRC is considered thought to contribute to clearance of natriuretic peptides from circulation,[22] circulating N-terminal pro B-natriuretic peptide NT-pro-BNP levels were measured in AKR and C3H mice fed high fat or control diets. From 0 to 20 weeks, only AKR mice fed high fat diet showed a decrease in circulating NT-pro-BNP levels, as expected with increased NPRC expression. Regardless of diet, C3H mice showed an increase in NT-pro-BNP after 20 weeks (Fig. 5a). Finally, to determine the extent to which other genes within the natriuretic peptide system were affected, RNA sequencing data demonstrated that
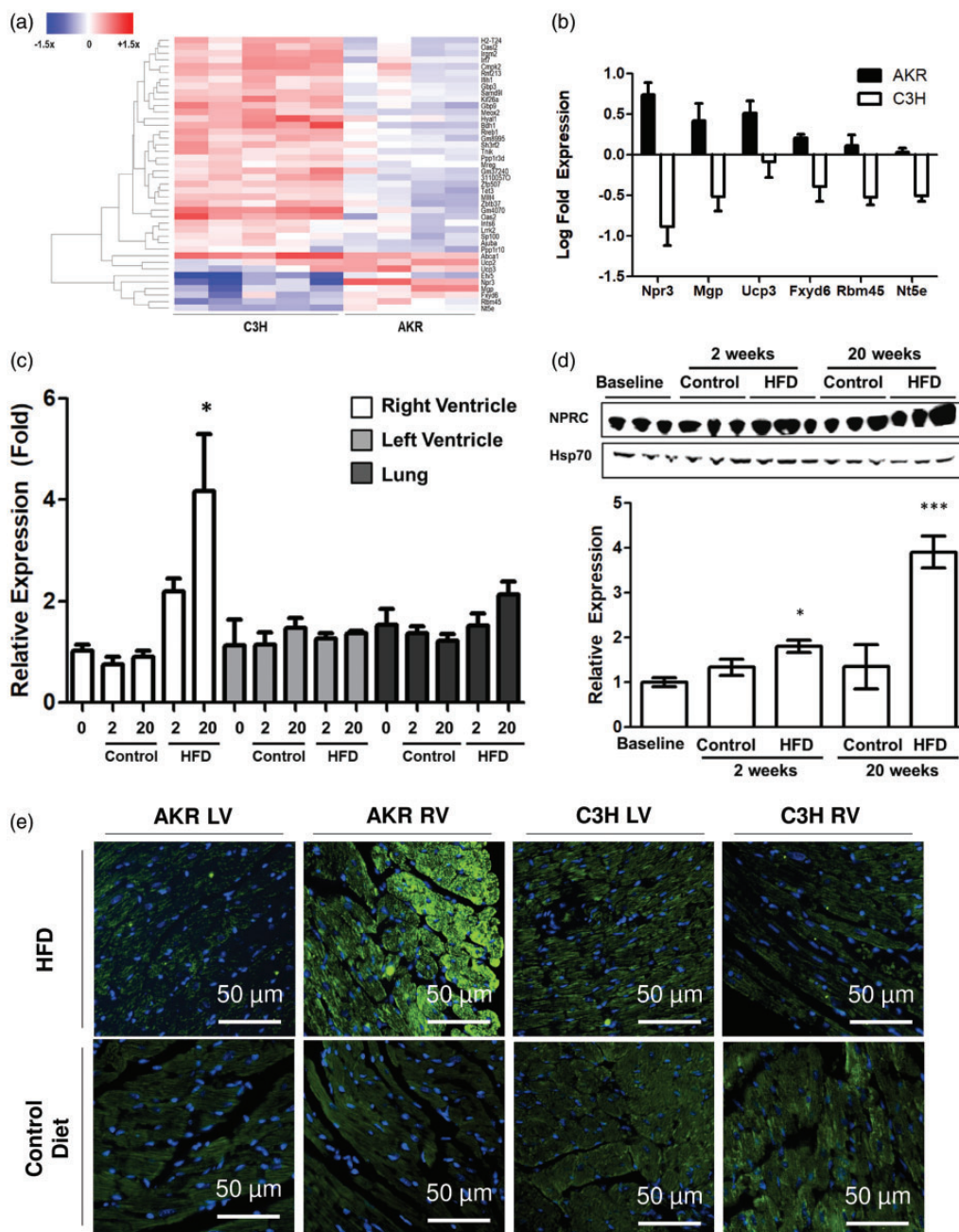

Fig. 4. (a and b) RNA sequencing of the right ventricle at two weeks post-diet identified differentially regulated genes between AKR and C3H mice, of which *NPRC* was the most differentially expressed. (c–e) RT-PCR, high fat blot, and immunostaining confirmed increased *NPRC* expression selectively in the right ventricle. *$p < 0.05$ and ***$p < 0.001$ compared to control. Data presented as mean $\pm$ SEM.
NPRC: natriuretic peptide clearance receptor C; HFD: high fat diet; RV: right ventricle; LV: left ventricle.
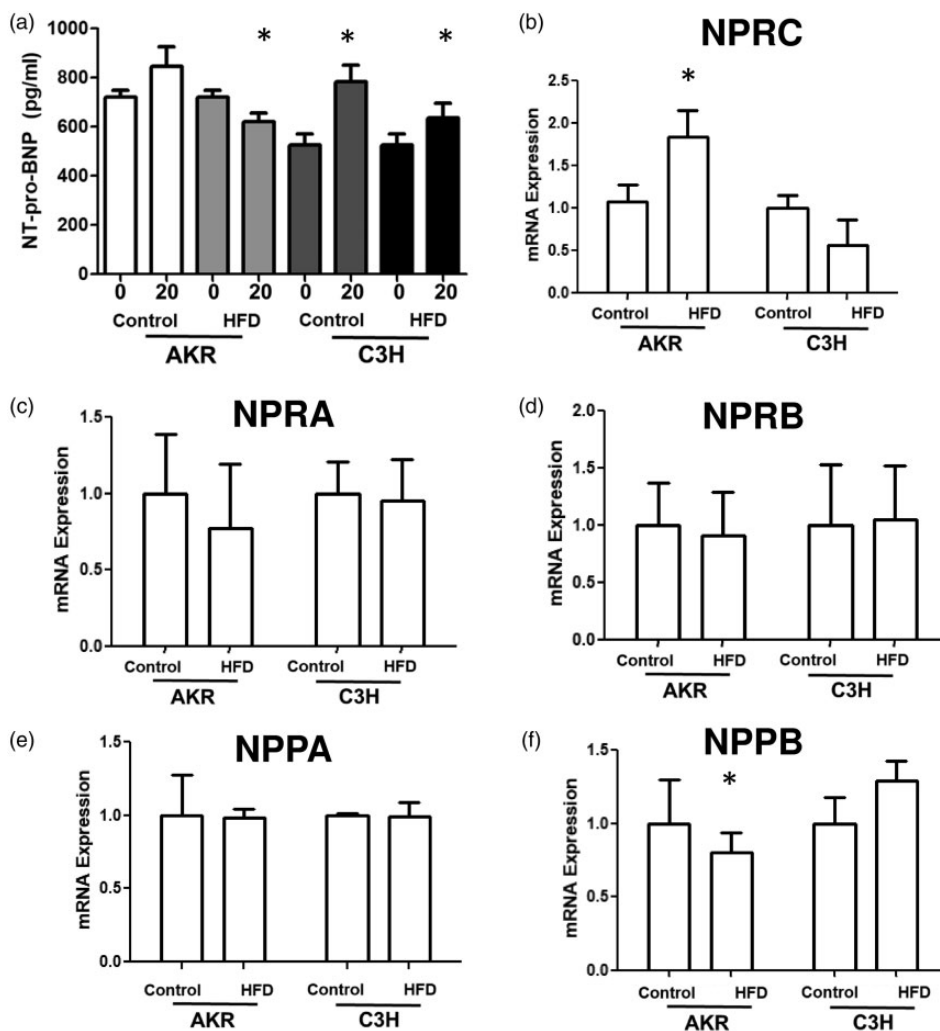
Fig. 5. (a) There is decreased circulating NT-pro-BNP in AKR mice fed a high fat diet. (b–f) RT-PCR expression of the right ventricle confirms that *NPRC* is the only gene in the natriuretic peptide system differentially expressed. *$p < 0.05$ compared to control. Data presented as mean ± SEM.

NPRC: natriuretic peptide clearance receptor C; HFD: high fat diet.

only one natriuretic peptide receptor, NPRC, and not NPRA or NPRB, was changed in expression in the RV of AKR mice fed high fat diet (Fig. 6b–d). Additionally, no change in expression of natriuretic peptide ANP (gene *NPPA*) was noted, but there was a decrease in BNP (NPPB) expression (Fig. 6e and f). Of note, expression of NPPC and neprilysin NEP) were not detected in sufficient quantities in the RV.

NPRC increases pathologic cell hypertrophy of cardiomyocytes in vitro

To determine the effect of NPRC upon cardiomyocyte hypertrophy, cardiomyocyte-like H9C2 cells were transduced with a plasmid containing either human NPRC or an empty vector. Transduced cells demonstrated an increase in in transcript expression of NPRC (Fig. 6a) and protein expression by both immunofluorescence and Western blot

(Fig. 6b). H9C2 cells overexpressing NPRC overall demonstrated an increase in cell size compared to empty vector controls (Fig. 6d). They also showed an increase in β-cardiac myosin heavy chain (*MYH7*) and atrial natriuretic peptide (*NPPA*), both genes activated in pathologic cardiomyocyte hypertrophy (Fig. 6e and f). Upon treatment with a selective ligand for NPRC, ANP-4-23,[21] cells overexpressing *NPRC* displayed a decrease in cell size (Fig. 7a) and decrease in expression of *MYH7* (Fig. 7b) but not *NPPA* (Fig. 7c).

Discussion

PH due to left heart disease, and specifically HFpEF, is a highly prevalent and morbid disease with no current therapeutic options to improve mortality. This is, in part, due to a lack of animal models that faithfully recapitulate features of HFpEF,[13] and a lack of understanding of the pathophysiology of RV dysfunction in the context of PH-HFpEF.
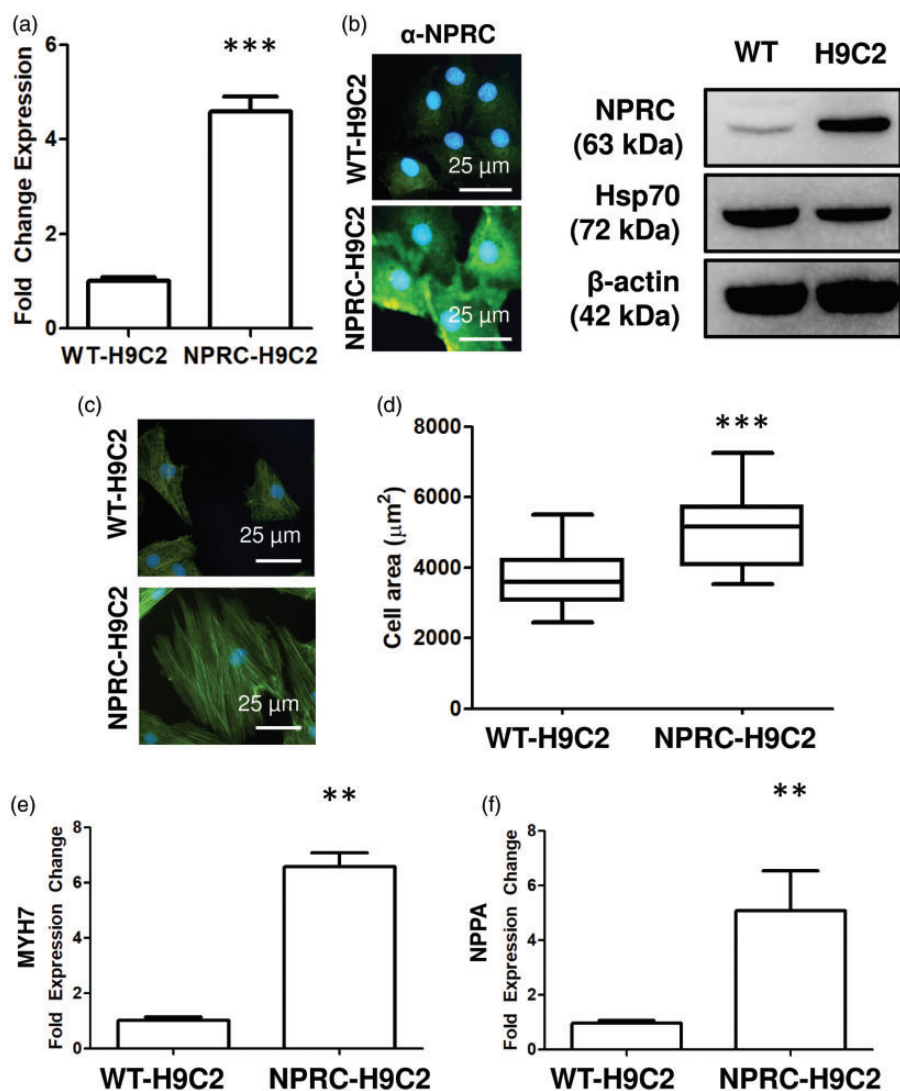
Fig. 6. (a) Confirmation of increased NPRC expression by PCR and immunofluorescence in transfected H9C2 cells. (B) Transfected H9C2 cells retain their ability to differentiate based on troponin stain. (c and d) Overexpression of *NPRC* in H9C2 causes increased cell hypertrophy based on increased cell size. (e) Increased expression of hypertrophic markers, MYH7 and NPPA in NPRC overexpressing H9C2 cells. *$p < 0.05$,**$p < 0.01$, and ***$p < 0.001$ compared to control. Data presented as either mean $\pm$ standard deviation or Tukey box-and-whisker plot. NPRC: natriuretic peptide clearance receptor C.

Given that obesity and metabolic syndrome are central to the pathogenesis of PH, RV dysfunction, and HFpEF,[8,23,24] our study validated and extended a relevant, obesity-induced model of PH and HFpEF to study the pathogenesis of RV dysfunction in HFpEF. Exploiting common genetic variation among available mouse strains to account for effects of diet alone, we identified genes uniquely contributing to the development of RV dysfunction in the context of obesity-induced PH-HFpEF. Of these genes, we identified a therapeutic target in natriuretic peptide receptor C, a clearance receptor for natriuretic peptide, and showed that it contributes to cardiomyocyte hypertrophy.

While our model shares many features with other models of HFpEF,[13,25–29] including the use of high fat diet in mice prone to development of metabolic syndrome,[30] our study is

unique in that it focused on RV dysfunction, a common cause of death in this patient population.[3,31–33] Using a relevant model of obesity-induced HFpEF, we found RV hypertrophy to be an early manifestation of disease in response to high fat diet in this model. Our model builds upon a previous study by Meng et al. that identified the AKR mouse strain as susceptible to high fat diet-induced hemodynamic and structural changes consistent with HFpEF and PH.[16] Our study shows very similar hemodynamic and structural changes in the heart and lung after 20 weeks of high fat diet compared to their study, including similar increases in RV systolic pressure measurement, left ventricular mass, RV mass, left ventricular end-diastolic pressure, and pulmonary vascular resistance. A key addition of our study is the finding of changes in RV mass as early as two weeks post-high
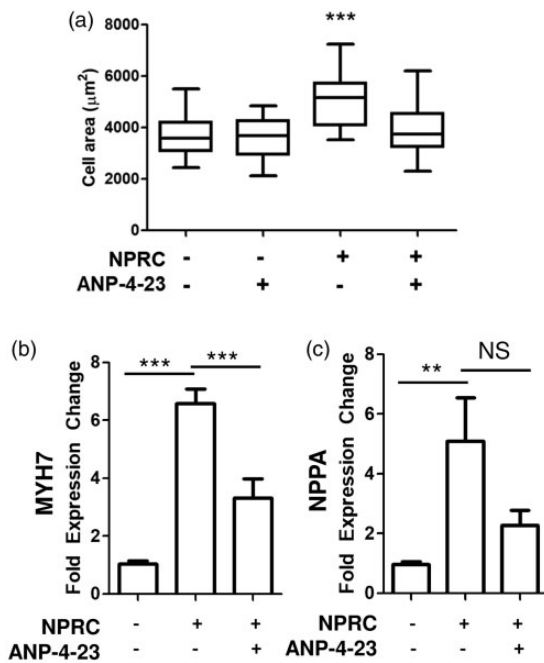
Fig. 7. (a) Treatment with NPRC-selective agonist, ANP-4-23, decreases cell size in NPRC transfected H9C2 cells, but not control H9C2 cells. (b) ANP-4-23 treatment decreases MYH7 expression in NPRC transfected H9C2 cells. (c) ANP-4-23 does not significantly decrease NPPA expression in NRPC transfected H9C2 cells. *$p < 0.05$, **$p < 0.01$ and ***$p < 0.001$ compared to control. Data presented as mean $\pm$ standard deviation or Tukey box-and-whiskey plot. NPRC: natriuretic peptide clearance receptor C.

fat diet change, a time point that was not reported by Meng et al. While the study by Meng et al. did report an increase in RV mass at eight weeks post-high fat diet, it is possible the differences in the compositions of control diets may account for the changes noted early in our study. While Meng et al. used standard chow as a control diet, our study utilizes a specially developed control diet that is calorie neutral and low in fat. Previous studies have shown that other nutrients such as proteins and carbohydrates can have profound effects upon myocardial remodeling,[25,34] and thus future studies may need to investigate specific differences in macronutrients that regulate RV remodeling. Additionally, despite observing a difference in RV mass after two weeks of high fat diet in AKR mice, our study did not show any evidence of changes in pulmonary vascular resistance after two weeks of high fat diet. However, our study was likely underpowered to detect smaller early differences in pulmonary vascular remodeling based on our numbers of animals per group.

HFpEF is recognized now to be a heterogeneous multisystem disorder as opposed to a singular disease entity,[35] and this heterogeneity has been considered a limitation in identifying effective therapies for this population thus far. Clinical studies have suggested that metabolic derangements such as diabetes mellitus, obesity, and metabolic syndrome may contribute to a unique phenotype within the population

of HFpEF that is characterized by disproportionate RV remodeling and PH.[14] Not only is body mass index independently associated with an increased risk for development of HFpEF but not systolic heart failure,[36] but obesity and metabolic syndrome are both independently associated with RV remodeling even in the absence of heart failure.[37,38] Our findings would suggest that NPRC expression may at least partially drive changes in the RV seen in patients in HFpEF patients with metabolic syndrome. Since NPRC's expression and function is integral to the development of metabolic syndrome,[39,40] our findings also support the emerging hypothesis that metabolic derangements may be a driver of HFpEF in certain subsets of patients. Future studies are necessary to directly test the extent to which NPRC is responsible for the HFpEF phenotype in patients with metabolic syndrome, though.

A key finding of our study identifies natriuretic peptide receptor C as possible contributor to RV hypertrophy. Our study shows an association between RV hypertrophy and increased NPRC expression in vivo, and both an increase in cell size and activation of a hypertrophic gene program in vitro. The natriuretic peptides are central mediators of the body's systemic response to increased ventricular strain, generally activating pathways that promote myocyte lusitropy, systemic vasorelaxation, and natriuresis to reduce strain upon the heart.[41] Recent studies, however, also suggest that natriuretic peptides play a prominent role in regulating obesity and metabolic syndrome.[40,42] Functioning through its two canonical receptors, NPRA and NPRB, natriuretic peptides have been found to increase mitochondrial biogenesis and prevent obesity in a guanosine monophosphate cGMP-dependent fashion.[43] The third receptor, NPRC, is a transmembrane membrane receptor similar to NPRA and NPRB, but has a short cytoplasmic tail lacking a guanylyl cyclase catalytic domain. While thought to be a "clearance receptor" that internalizes natriuretic peptides, studies have shown that it can also directly alter signaling through inhibition of adenylyl cyclase and adenosine cyclic 3'5'-monophosphate cAMP production via pertussis-sensitive Gi protein.[44] Additionally, genetic knockout of NPRC restores natriuretic responsiveness in adipose tissue to reduce insulin resistance and obesity.[40] The finding that a receptor that regulates activity and function of circulating natriuretic peptides may be important in the pathogenesis of PH-HFpEF and RV dysfunction is consistent with the growing perception that both HFpEF and PH are organ-specific manifestations of systemic derangements.[45,46]

This study has a number of limitations. The two mouse strains differ genetically in a number of ways, and thus there are many genetic differences between the two mouse strains that could have given rise to a differential response to PH-HFpEF and RV dysfunction. Even in the current study, a total of 42 genes were noted to be differentially regulated between AKR and C3H mice in the RV in response to high fat diet. Of them, NPRC was chosen for further study given its known connection to heart failure, PH, metabolic

syndrome, and obesity.[22,40] However, contribution of other gene pathways cannot be ruled out in our model from the current study alone.

Our study specifically used male mice for the current study, and thus whether these findings apply to female mice is not clear. Male mice for the current study were chosen because most contemporary studies suggest that obesity-related HFpEF is primarily a disease of men and post-menopausal women.[47] To eliminate the confounding effect that sex-based differences play in the development of HFpEF,[5] male mice were chosen for this study. Future studies will directly investigate the effect of high fat diet upon development of PH-HFpEF in female AKR mice, as well as female AKR mice that have undergone bilateral oophorectomy.

This study also focused on the role of NPRC in cardiomyoblast cells in vitro. It is possible that NPRC could be exerting a pro-hypertrophic effect through non-cardiomyocyte cells in vivo, such as fibroblasts, smooth muscle cells, or endothelial cells. While future studies are needed to directly assess the effect of NPRC expression in these other cell populations, and secondarily any effects that these other cell populations may then have on cardiomyocyte function, our study suggests that NPRC may at least have a direct effect upon cardiomyocyte hypertrophy through increased expression in cardiomyocytes.

Finally, the present study identified NPRC as a potential contributor to RV hypertrophy in a relevant in vivo and in vitro model. However, it is not clear mechanistically whether this is a function of NPRC competing for endogenous natriuretic peptides and limiting signaling through other receptors, or whether this is directly the result of signaling downstream of NPRC.[22,44] Future studies are needed to better understand precisely how NPRC affects development of RV hypertrophy by further understanding its direct and indirect role in RV pathophysiology.

In conclusion, our study validates and extends a highly relevant model of diet and obesity-induced PH-HFpEF to identify *NPRC* expression as uniquely increased in the right ventricle of mice that develop PH-HFpEF. In vitro, *NPRC* overexpression results in an increase in cardiomyocyte cell size and activation of gene programs consistent with pathologic cell hypertrophy. While future studies are necessary to further investigate the precise mechanisms by which NPRC is activated and contributes to cardiac hypertrophy of the RV, the findings of the present study suggest that NPRC is a promising therapeutic target in RV dysfunction in the setting PH-HFpEF.

Author contributions

V.A. conceived idea, carried out experiments, and wrote the manuscript; N.F., S.Y., J.F, F.S., D.N., L.G., and E.P. carried out experiments, performed analytic calculations, and provided critical feedback in research and manuscripts; T.J.W, E.L.B., and S.C. contributed to design and implementation of research, provided critical feedback in research and manuscripts; J.D.W. and A.R.H. conceived idea, contributed to design and implementation of research, and provided critical feedback in research and manuscripts.

ORCID iD

Vineet Agrawal https://orcid.org/0000-0002-8457-6722

References

1. Hoeper MM, Humbert M, Souza R, et al. A global view of pulmonary hypertension. *Lancet Respir Med* 2016; 4: 306–322.
2. Chatterjee NA, Steiner J and Lewis GD. It is time to look at heart failure with preserved ejection fraction from the right side. *Circulation* 2014; 130: 2272–2277.
3. Lam CSP, Roger VL, Rodeheffer RJ, et al. Pulmonary hypertension in heart failure with preserved ejection fraction: a community-based study. *J Am Coll Cardiol* 2009; 53: 1119–1126.
4. Melenovsky V, Hwang S-J, Lin G, et al. Right heart dysfunction in heart failure with preserved ejection fraction. *Eur Heart J* 2014; 35: 3452–3462.
5. Duca F, Zotter-Tufaro C, Kammerlander AA, et al. Gender-related differences in heart failure with preserved ejection fraction. *Sci Rep* 2018; 8: 1080.
6. Lehto H-R, Lehto S, Havulinna AS, et al. Does the clinical spectrum of incident cardiovascular disease differ between men and women?. *Eur J Prev Cardiol* 2014; 21: 964–971.
7. Meoli DF, Su YR, Brittain EL, et al. The transpulmonary ratio of endothelin 1 is elevated in patients with preserved left ventricular ejection fraction and combined pre- and post-capillary pulmonary hypertension. *Pulm Circ* 2018; 8: 2045893217745019.
8. Fayyaz AU, Edwards WD, Maleszewski JJ, et al. Global pulmonary vascular remodeling in pulmonary hypertension associated with heart failure and preserved or reduced ejection fraction. *Circulation* 2018; 137: 1796–1810.
9. Califf RM, Adams KF, McKenna WJ, et al. A randomized controlled trial of epoprostenol therapy for severe congestive heart failure: the Flolan International Randomized Survival Trial (FIRST). *Am Heart J* 1997; 134: 44–54.
10. Packer M, McMurray JJV, Krum H, et al. Long-term effect of endothelin receptor antagonism with bosentan on the morbidity and mortality of patients with severe chronic heart failure: primary results of the ENABLE trials. *JACC Heart Fail* 2017; 5: 317–326.
11. Redfield MM, Chen HH, Borlaug BA, et al. Effect of phosphodiesterase-5 inhibition on exercise capacity and clinical status in heart failure with preserved ejection fraction. *JAMA* 2013; 309: 1268.
12. Reddy S and Bernstein D. Molecular mechanisms of right ventricular failure. *Circulation* 2015; 132: 1734–1742.
13. Valero-Muñoz M, Backman W and Sam F. Murine models of heart failure with preserved ejection fraction: a "Fishing Expedition". *JACC Basic Transl Sci* 2017; 2: 770–789.
14. Obokata M, Reddy YNV, Pislaru SV, et al. Evidence supporting the existence of a distinct obese phenotype of heart failure with preserved ejection fraction. *Circulation* 2017; 136: 6–19.

15. Ho JE, Enserro D, Brouwers FP, et al. Predicting heart failure with preserved and reduced ejection fraction: the international collaboration on heart failure subtypes. *Circ Hear Fail* 2016; 9: e003116.

16. Meng Q, Lai Y-C, Kelly NJ, et al. Development of a mouse model of metabolic syndrome, pulmonary hypertension, and heart failure with preserved ejection fraction. *Am J Respir Cell Mol Biol* 2017; 56: 497–505.

17. Brittain E, Penner NL, West J, et al. Echocardiographic assessment of the right heart in mice. *J Vis Exp* 2013; 27: e50912.

18. Chemla D, Humbert M, Sitbon O, et al. Systolic and mean pulmonary artery pressures. *Chest* 2015; 147: 943–950.

19. Parker JC and Townsley MI. Evaluation of lung injury in rats and mice. *Am J Physiol Cell Mol Physiol* 2004; 286: L231–L246.

20. Hemnes AR, Brittain EL, Trammell AW, et al. Evidence for right ventricular lipotoxicity in heritable pulmonary arterial hypertension. *Am J Respir Crit Care Med* 2014; 189: 325–334.

21. Schmitt M, Qasem A, McEniery C, et al. Role of natriuretic peptides in regulation of conduit artery distensibility. *Am J Physiol Circ Physiol* 2004; 287: H1167–H1171.

22. Matsukawa N, Grzesik WJ, Takahashi N, et al. The natriuretic peptide clearance receptor locally modulates the physiological effects of the natriuretic peptide system. *Proc Natl Acad Sci USA* 1999; 96: 7403–7408.

23. Friedman SE and Andrus BW. Obesity and pulmonary hypertension: a review of pathophysiologic mechanisms. *J Obes* 2012; 2012: 1–9.

24. Haque AK, Gadre S, Taylor J, et al. Pulmonary and cardiovascular complications of obesity: an autopsy study of 76 obese subjects. *Arch Pathol Lab Med* 2008; 132: 1397–1404.

25. Carbone S, Mauro AG, Mezzaroma E, et al. A high-sugar and high-fat diet impairs cardiac systolic and diastolic function in mice. *Int J Cardiol* 2015; 198: 66–69.

26. Christopher BA, Huang H-M, Berthiaume JM, et al. Myocardial insulin resistance induced by high fat feeding in heart failure is associated with preserved contractile function. *Am J Physiol Circ Physiol* 2010; 299: H1917–H1927.

27. Huang J-P, Cheng M-L, Wang C-H, et al. High-fructose and high-fat feeding correspondingly lead to the development of lysoPC-associated apoptotic cardiomyopathy and adrenergic signaling-related cardiac hypertrophy. *Int J Cardiol* 2016; 215: 65–76.

28. Leopoldo AS, Sugizaki MM, Lima-Leopoldo AP, et al. Cardiac remodeling in a rat model of diet-induced obesity. *Can J Cardiol* 2010; 26: 423–429.

29. Schiattarella GG, Altamirano F, Tong D, et al. Nitrosative stress drives heart failure with preserved ejection fraction. *Nature* 2019; 568: 351–356.

30. Tang Y, Ho G, Li Y, et al. Beneficial metabolic effects of CB1R anti-sense oligonucleotide treatment in diet-induced obese AKR/J mice. *PLoS One* 2012; 7: e42134.

31. Mohammed SF, Hussain I, AbouEzzeddine OF, et al. Right ventricular function in heart failure with preserved ejection fraction. *Circulation* 2014; 130: 2310–2320.

32. Guazzi M, Dixon D, Labate V, et al. RV contractile function and its coupling to pulmonary circulation in heart failure with preserved ejection fraction: stratification of clinical phenotypes and outcomes. *JACC Cardiovasc Imaging* 2017; 10: 1211–1221.

33. Aschauer S, Zotter-Tufaro C, Duca F, et al. Modes of death in patients with heart failure and preserved ejection fraction. *Int J Cardiol* 2017; 228: 422–426.

34. Bostick B, Habibi J, DeMarco VG, et al. Mineralocorticoid receptor blockade prevents Western diet-induced diastolic dysfunction in female mice. *Am J Physiol Circ Physiol* 2015; 308: H1126–H1135.

35. Parikh KS, Sharma K, Fiuzat M, et al. Heart failure with preserved ejection fraction expert panel report: current controversies and implications for clinical trials. *JACC Hear Fail* 2018; 6: 619–632.

36. Savji N, Meijers WC, Bartz TM, et al. The association of obesity and cardiometabolic traits with incident HFpEF and HFrEF. *JACC Hear Fail* 2018; 6: 701–709.

37. Gopal DM, Santhanakrishnan R, Wang Y-C, et al. Impaired right ventricular hemodynamics indicate preclinical pulmonary hypertension in patients with metabolic syndrome. *J Am Heart Assoc* 2015; 4: e001597.

38. Wong CY, O'Moore-Sullivan T, Leano R, et al. Association of subclinical right ventricular dysfunction with obesity. *J Am Coll Cardiol* 2006; 47: 611–616.

39. Coué M, Barquissau V, Morigny P, et al. Natriuretic peptides promote glucose uptake in a cGMP-dependent manner in human adipocytes. *Sci Rep* 2018; 8: 1097.

40. Wu W, Shi F, Liu D, et al. Enhancing natriuretic peptide signaling in adipose tissue, but not in muscle, protects against diet-induced obesity and insulin resistance. *Sci Signal* 2017; 10: eaam6870.

41. Volpe M, Rubattu S, Burnett J, et al. Natriuretic peptides in cardiovascular diseases: current use and perspectives. *Eur Heart J* 2014; 35: 419–25.

42. Wang TJ, Larson MG, Levy D, et al. Impact of obesity on plasma natriuretic peptide levels. *Circulation* 2004; 109: 594–600.

43. Miyashita K, Itoh H, Tsujimoto H, et al. Natriuretic peptides/cGMP/cGMP-dependent protein kinase cascades promote muscle mitochondrial biogenesis and prevent obesity. *Diabetes* 2009; 58: 2880–2892.

44. Anand-Srivastava MB, Sehl PD and Lowe DG. Cytoplasmic domain of natriuretic peptide receptor-C inhibits adenylyl cyclase. Involvement of a pertussis toxin-sensitive G protein. *J Biol Chem* 1996; 271: 19324–19329.

45. Packer M and Kitzman DW. Obesity-related heart failure with a preserved ejection fraction. *JACC Hear Fail* 2018; 6: 633–639.

46. Hemnes AR and Humbert M. Pathobiology of pulmonary arterial hypertension: understanding the roads less travelled. *Eur Respir Rev* 2017; 26: 170093.

47. Shah KS, Xu H, Matsouaka RA, et al. Heart failure with preserved, borderline, and reduced ejection fraction. *J Am Coll Cardiol* 2017; 70: 2476–2486.